Memoirs of the School of Engineering, Okayama University, Vol. 15-2, March 1981

Accuracy and Etalon Fringe Phenomena in Methane-gas Spectrometry Employing Tunable Diode Lasers

Ryuji KOGA*, Satoru NAGASE*,
Megumi KOSAKA*, Hiroya SANO*

Synopsis

A method to monitor atmospheric gas concentration employing a tunable diode laser is proposed. An apparatus was built and experiments were made. The tunable diode laser employed was of PbSnTe with its wavenumber about 1200 cm^{-1} at a temperature of 77 K. Methane concentration in laboratory atmosphere was measured on the experiments.

The inquired gas-density is obtained by a hard-wired microcomputer incorporating the measured absorption spectrum over a prescribed range instead of an absorption at a single wavenumber. By this, drift type noises are suppressed. After an analysis based on experimental data, an attainable sensitivity for methane was found to be 1 ppb·m. This value may increase if an etalon fringe interference exists. The natural concentration, about 1 ppm, of atmospheric methane was actually measured with a short optical path of only one meter.

1. Introduction

A gas monitoring scheme that is sensitive, local, real-time, *in situ* and portable is still required. Optical methods have been regarded as a superior alternative of traditional and proven chemical methods. They are slow and susceptible to different gas species, though they

* Department of Electronics.

are economic and sensitive. A non-dispersive infrared gas-analyzer[1] has been appreciated for its relatively high performance to its simple mechanism which allows reliable and economic operation. Efforts have been made to improve its sesitivity and selectivity adding a dispersive elements[2]. But the low luminescence of an infrared light source has limited the performance, so far.

A lead-salt diode laser has a fine and fast tunability in addition to many features common to other lasers. Employing this tunable diode laser(TDL) instead of a bulky and heavy monochrometer, one can expect to realize a compact and portable equipment[3][4].

This report is on the system for atmospheric gas analysis exploiting features of the TDL. A system configuration was proposed, and an experimental apparatus was built. After that, an attainable accuracy was analyzed on the basis of the results of experiments.

2. Principles

The principle of the gas concentration measurement is based on Lambert-Beer's law. Powers, P_O and P_I of an optical beam before and after the absorbing media of length L, respectively, are related by an equation,

$$P_I = P_O e^{-\tau}. \tag{1}$$

The attenuation for the light, τ, is further described as

$$\tau(\nu) = \eta + \alpha(\nu) c L, \tag{2}$$

where η stands for the attenuation by the equipment. Terms α, and c are the absorption coefficient as a function of the wavenumber of the light, ν, concentration of the inquired gas species, respectively. If this absorption spectrum $\tau(\nu)$ is obtained, one can calculate the density c by a mathematical expression

$$c = \frac{1}{L} l[D_2(\tau)], \tag{3}$$

where l is a functional, and D_2 is a linear operator, though this expression is too abstract. It has been known that a derivative spectrum is more distinct between gas species, and is profittable to discern a sharp but weak absorption line from a strong but gently

sloping base spectrum[5∿7]. The operator D_2 stands for the signal processing to obtain the $2f$-spectrum, S, which is equivalent to a second derivative of the crude absorption spectrum under a restricted condition. As is concluded in a Hilbert's space theory, the functional l is described with an inner product between S and another spectrum, w, viz.,

$$l[S(\nu)] = \langle S(\nu), w(\nu) \rangle . \tag{4}$$

By choosing w so that an orthogonality relation

$$\langle w, \eta \rangle = 0 \tag{5}$$

may hold, the inquired concentration c can be calculated by

$$c = \frac{1}{L} \frac{\langle w, S \rangle}{\langle w, \gamma \rangle} , \tag{6}$$

where $\gamma=\gamma(\nu)$ is a $2f$-spectrum of $\alpha(\nu)$.

An artifice to obtain the spectrum $S(\nu)=D_2(\tau)$ is described in Fig.1, which employs a pair of one TDL and an infrared detector(IRD). Output electronic signal is transferred to a lock-in-amplifier(LIA), and also to a pulse-height detector. They produce $P_0 D_2(\tau)$ and P_0, respectively. A normalization is carried out by a microcomputer[9].

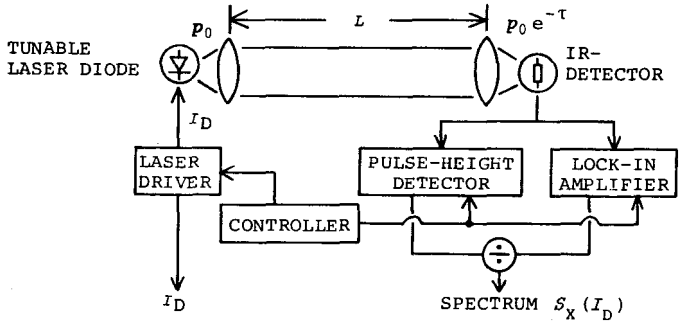

Fig.1 A single beam system. A $2f$-spectrum normalized by the IRD input is obtained.

If the spectra are based on the wavenumber, ν, the concentration calculation Eq.(3), may succeed. A tunable diode laser is, however, controlled of its ν by means of the change of the driving current, I_D. The correspondence of ν and I_D are not always unique, but is affected by a heat-sink temperature. Moreover, a TDL may emitt lights of different ν's at the same time, and fractions of their powers are also susceptible to the heat-sink temperature drift. The apparent spectrum $S(I_D)$ may change at different occasions, and the absolute spectrum $\alpha(\nu)$ specific to the inquired gas species is not available.

In order to avoid this difficulty, an alternative double beam system of Fig.2 were proposed and built. A portion of the light beam emitted from a TDL is divided by a beam splitter(BS), passes through a gas cell which contains a standard gas of the inquired species with known concentration, and impinges to an infrared-detector(IRD). This constitutes a reference leg(R-leg). Resultant portion of the beam runs through the atmosphere under the test or through a sample cell, impinging into another IRD: a leg for measurement(X-leg).

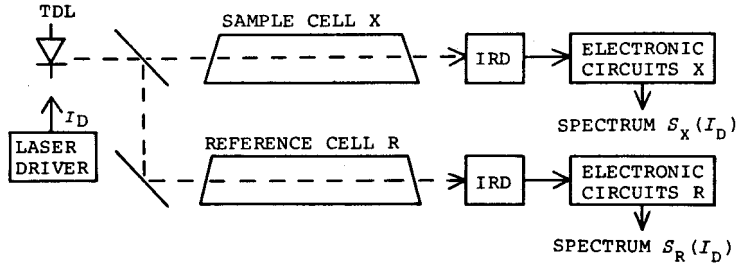

Fig.2 A double beam system to overcome the spectral uncertainty of TDL.

Two spectra S_R and S_X are obtained by exclusively prepared electronic circuits for each of the two IRD's. Basically, the two spectra are the same in their shapes but different only in its magnitudes. Namely, an equation

$$\frac{1}{c_X L_X} S_X(I_D) = \frac{1}{c_R L_R} S_R(I_D) \tag{7}$$

hold, where c_X, L_X and c_R, L_R are gas concentrations and optical paths of the X-leg and the R-leg, respectively. The inquired density is calculated by

$$c_X = \frac{c_R L_R}{L_X} \frac{\langle w, S_X \rangle}{\langle w, S_R \rangle} . \tag{8}$$

Here it should be noted that spectra, w, S_R, and S_X participating in Eq.(8) are functions of the TDL driving current, I_D, whereas those in Eq.(6), of the wavenumber, ν.

The weight w is chosen so that the functional of S, Eq.(8), is less sensitive to a prescribed and probable spectral interferences. This is possible by employing the notion of adjoint spectra[8]. Actually, the weight can be generated by the following equations

$$w = S_R - \sum_{i=1}^{I} \langle S_R, U_i \rangle U_i , \tag{9}$$

where U_i, $i=1,\cdots,I$ are the prescribed ortho-normalized spectra which correspond to the base-line shift, its tilt and/or its bucklings. The inner product $\langle \cdot, \cdot \rangle$ can be described as

$$\langle x, y \rangle = x^t Q y \tag{10}$$

employing a positive-definite, symmetric matrix Q, in our case, because a spectrum is expressed as a set of data of a definite number, a vector The employed matrix, Q, stands for a low-pass numerical filter or for a smoothing process.

Numerical calculations in the micro-computer are carried out with an equation

$$C_X = \frac{C_R L_R}{L_X} \frac{(S_R^*, S_X)}{(S_R^*, S_R)} , \tag{11}$$

where the notation $(\cdot, \cdot)$ stands for the ordinary inner product of two vectors, and S_R^*, an adjoint spectrum of S_R given by smoothing w, being described as

$$S_R^* = Qw. \tag{12}$$

As can easily be expected, an etalon fringe(EF) has a periodic structure, and has a sharp and discrete line shape in its Fourier transform. The suppression of EF can be done by this spectral distribution of the EF, which is characterized by a difference of the two optical paths along which the optical interference takes place.

3. Experimental Apparatus

Fig.3 is the schematic diagram of the experimental apparatus. Optical configuration is almost the same with Fig.2, but only two apertures are added. The employed laser element operates in multiple transversal modes and the emitting pattern has multiple sidelobes, which are different in wavenumbers. Apparent spectra of the two legs differ each other though they should be the same, because the dividing ratio of the beam splitter depends on the polarization angle and because of a selective vignetting for one leg, both of which result in the difference of colours. Employing the apertures, this difficulty can be reduced. Gas cell of 15cm length with BaF_2 windows and 10cm length, Si windows were used.

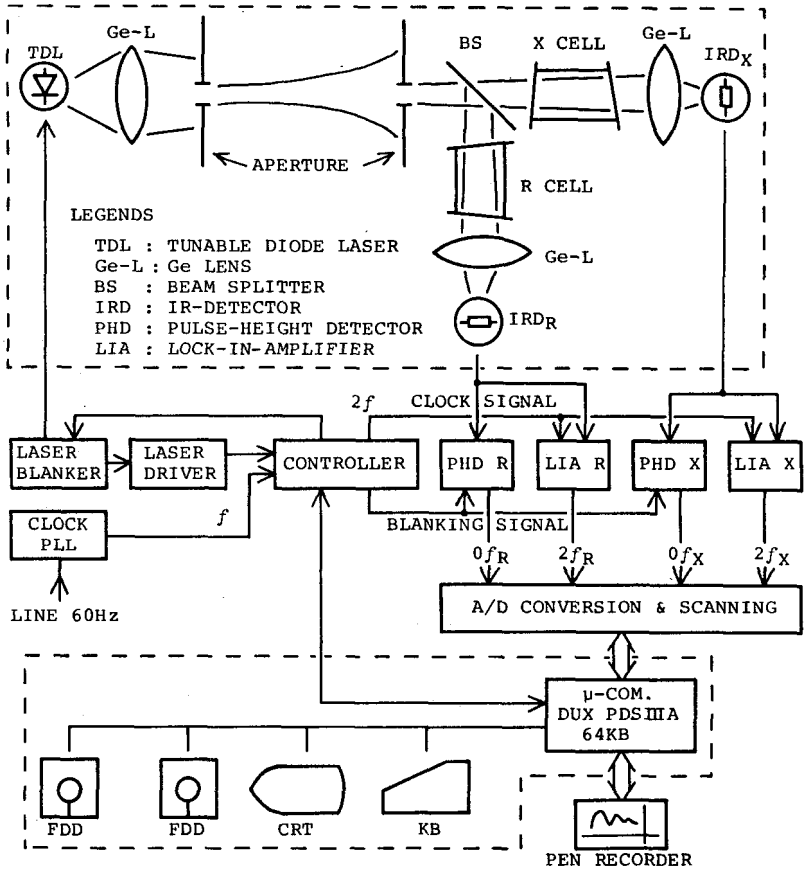

Fig.3 A schematic diagram of the experimental apparatus.

Signals from the IRD's are processed by lock-in-amplifiers and pulse-height detectors so that $2f$-signals $P_X S_X$, $P_R S_R$, and pulse heights P_X, P_R are yielded, respectively. These analog data are converted to digital data, scanned and transferred to the micro-computer system. The computer is based on Z80 CPU and is designed as a microcomputer-developing tool, equipped with 64KB RAM, two diskette drives(FDD), a CRT display and a key-board(KB). A spectrum stored in the computer in a digital form can be reversely converted to an analog signal and is drawn with a pen-recorder. A pair of R- and X-spectra, each of which is composed of 256 data of 8 bits, are scanned over four seconds, and is stored in the diskette. The gas concentration reductions are made afterwards. Major parameters of the TDL is listed in Table 1.

Table 1 Parameters of the employed tunable diode laser.

Constituents	PbSnTe
Wavenumber region (Wavelength)	≈1280 cm^{-1} at 77K (7.9 μm)
Lasing threshold	350 mA
Maximum drive current	900 mA
Tuning rate	0.01∿0.015 cm^{-1}/mA
Power	≤100 μW
Lasing mode	Multiple both transversally and longitudinally.

4. Experimental results

Fig.4 is a spectra pair of methane of 1 atm and 3 Torr. By this figure, the spectra of 1 atm is solely attributed to methane. Equating both pressures, a spectra pair of Fig.5 was obtained. This is a result of a fine adjustment of the apertures in Fig.3. A line designated by the asterisc(*) in both Fig.3 and Fig.4 are considered to belong to a mode different from others. Shapes of the spectra of Fig.4 is slightly different at marked positions. Fig.6 is a result of the gas concentration calculation employing Eq.(11), where the smoothing matrix Q is taken as a unit matrix and only one spectrum in Eq.(9) is employed to eliminate the base-line shift. Spectra pairs were taken every one minute over 20 minutes. Resultant density value changes as the time elapses. Associated marks, N15∿N39, are names of the recorded data-files stored in the diskette. Corresponding to these marked points, the spectra pairs are illustrated in Fig.7. Evidently, shapes of two

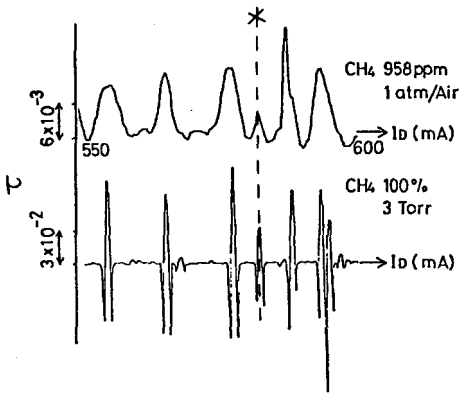

Fig.4 A spectra pair of methane taken with the system of Fig.3. Line widths differ because of pressure difference.

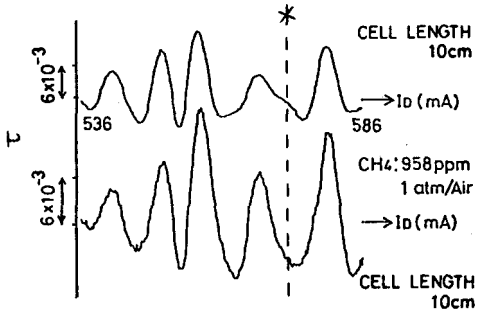

Fig.5 A spectra pair of methane of the same pressure. The marked line is due to a different mode of TDL output.

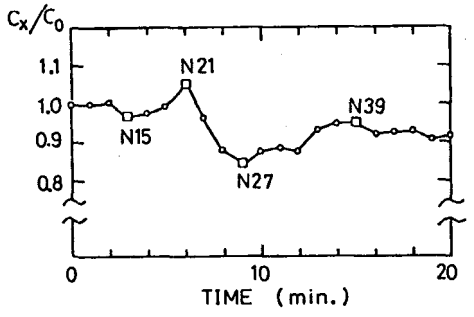

Fig.6 Measured gas concentrations. Associated numbers are the file numbers in the computer.

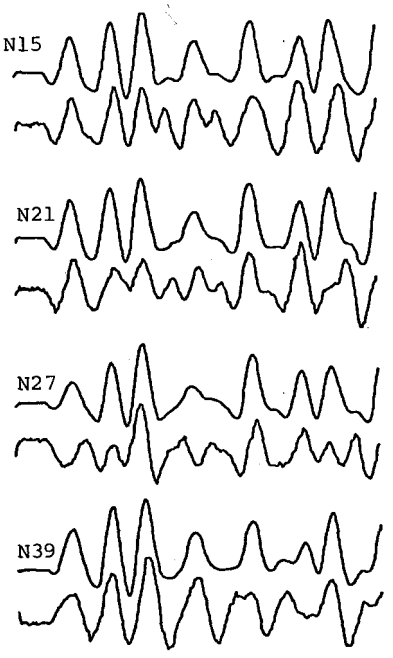

Fig.7 (Right) Some spectra pairs corresponding to the marked data of Fig.6. Difference in shapes are found and this is the cause of the concentration variation.

spectra of each pair are changing on time. This was attributed to the transversely-multimode oscillation of the TDL and an irregular multiple internal reflection in the reference cell with Si windows which have strong surface reflection.

Fig.8 is an example of an etalon fringe which may be the dominant spectral noise. Fig.9 is its Fourier transform, which is described in an amplitude (a) and a phase (b). The Fourier fransform is a function of the spectral frequency, corresponding to a difference between two optical paths, d, along which the lights from the same source travel and interfere.

As has been found in the reference[9], this fringe moves back and forth in time only in phase keeping its amplitude almost constant. Fig.10 is a temporal trace of the Fourier coefficients at d=16.1 cm. From this, it is found that this coefficients are composed of two components: one is almost constant both in the phase and the amplitude, and another, constant in amplitude but its phase monotonically increases. This monotonic increase in phase is attributed to the thermal expansion of a Dewar vessel which was used to keep the liquid nitrogen in order to cool and support the TDL element at the temperature of 77K, since the increment of the phase $\delta\vartheta$ and the increase in the optical-path difference, δd, is related by an equation

$$\delta\vartheta = 2\pi\nu(\delta d), \tag{13}$$

where ν is the wavenumber.

5. Analysis of the Accuracy

Probable noise sources are listed in Table 2. Refferring to Eq.(1), a precise error analysis is made here. The two spectra S_X and S_R are expressed as

$$S_X = \frac{1}{P_X} D_2[\delta P_O] + D_2[\delta\tau_X] \tag{14}$$

$$S_R = D_2[\delta\tau_R] \tag{15}$$

where δP_O, $\delta\tau_X$ and $\delta\tau_R$ stand for components of P_O, τ_X and τ_R which survive the filtering operation of lock-in-amplifiers, respectively.

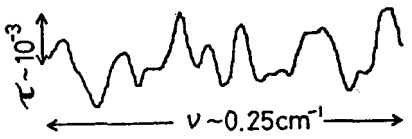

Fig.8 An example of etalon fringe.

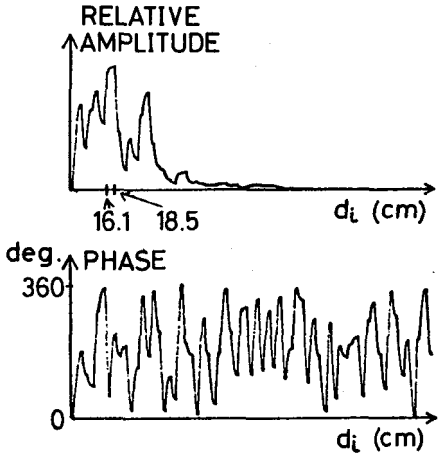

Fig.9 Fourier transform of the fringe spectrum of Fig.8. These spectra are functions of spectral frequency or an optical-path difference.

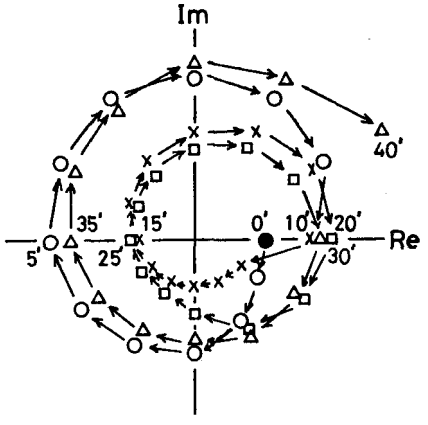

Fig.10 A temporal change of an etalon fringe mode of d=16.1 cm of Fig.9. Monotonic increase in phase is found though not in the amplitude.

Table 2 Possible noise sources.

Terms	Statistical features	Suppressibility by the numerical treatise, Eq.(11)
Spectral interference due to other gas	occasional	○
Kink in laser power	drift	○
Window contamination	drift	◎
Etalon fringes	drift	○
Random noises		
Infrared detector, Electronic circuits	random	×
Quantization noise	quasi random	×

Supressed; very well, ◎: well, ○: not supressed, ×

The first term in the right of Eq.(14) is due to the "kink" characteristic of TDL in the output power as a function of the driving current. In S_R of Eq.(15), the signal $\delta\tau_R$ is enough strong because of the high concentration-length product, $c_R L_R$, of the reference gas cell, and the kink signal term can be ignored. The absorption spectrum $\delta\tau_X$ is composed of the gas absorption, etalon fringes and random noise, viz.,

$$\delta\tau_X = \frac{1}{P_X}\sum_i \alpha(\nu_i)P_i + \sum_i\sum_l \{\varepsilon_l \cos(2\pi d_l \nu_i + \vartheta_l)\} + N, \tag{16}$$

$$\nu_i = \nu_i(I_D), \tag{17}$$

where the index i spans over the LTD modes, and l, the Fabry-Perot modes of etalon fringes, and N stands for the random noise converted into the equivalent attenuation. A variation of N is obtained after some calculations as

$$\sigma^2(N) = \frac{1}{P_X^2}\left\{\frac{A_D}{(D^*)^2} + \frac{e_n^2}{G^2}\right\}\frac{\pi}{T}, \tag{18}$$

where T is the time period over which an integrator of the phase sensitive detector operates and one datum is obtained. Other symbols are assigned as,

A_D: Detector area of IRD,
D^*: The detectivity of IRD compensated by A_D,
G : Sensitivity of IRD,
e_n: Noise-equivalent input rms-voltage of the electronic system.

Errors in the calculated gas concentration c are,
for the TDL kink,

$$\delta c_R = \frac{c_R L_R}{L_X} \frac{(S_R^*,\ D_2[\delta P_O])}{(S_R^*,\ S_R)} \tag{19}$$

for the etalon fringes,

$$\delta c_e = \frac{c_R L_R}{L_X} \frac{\sum_{il} \varepsilon_l (S_R^*, \cos\{2\pi d_l \nu_i + \vartheta_l\})}{(S_R^*,\ S_R)}\ , \tag{20}$$

and for the random noise,

$$\sigma(\delta c_n) = \frac{c_R I_R}{L_X P_X} \frac{\sqrt{(S_R^*,\ S_R^*)}}{(S_R^*,\ S_R)} \sqrt{\{\frac{A_D}{(D^*)^2} + \frac{e_n^2}{G^2}\} \frac{\pi}{TM}}\ , \tag{21}$$

where M is the number of data constituting a spectrum.

Table 3 Parameters for noise analysis.

A_D	0.01 cm^2	L_R	10 cm
D^*	1.6×10^{10} $cm\sqrt{Hz}/W$	L_X	100 cm
G	300 V/W	e_n	4 $nV/\sqrt{Hz}$
T	16.7 ms	ε	1.2×10^{-3}
M	128	P_X	100 μW
c_R	958 ppm	$(S_R^*,\ S_R)$	10^{-3}
		$(S_R^*,\ S_R^*)$	3×10^{-3}

In order to know the attainable sensitivity, some of these parameters should be estimated. The kink signal arises from the multimodal operation of TDL and is expected to be reduced to a very low level if a signal mode operation is achieved. Amplitude of an etalon fringe, ε, is convinced to be some orders below the square of the reflectance of the surfaces. Employing anti-reflection coatings and Brewster's angle, magnitude of ε would be less than 10^{-4} or possibly 10^{-6}. Other parame-

ters should be estimated. The kink signal arises from the multimodal operation of TDL and is expected to be reduced to a very low level if a signal mode operation is achieved. Amplitude of an etalon fringe,ε, is convinced to be some orders below the square of the reflectance of the surfaces. Employing anti-reflection coatings and Brewster's angle, magnitude of ε would be less than 10^{-4} or possibly 10^{-6}. Other parameters can be measured for the employed elements as shown in Table 3. Results are, $\sigma(\delta c_n)=1.1\times10^{-2}$[ppm] and $\delta c_e \simeq 0.3$[ppm]. The kink signal on our experiments was below the atmospheric methane concentration of some ppm's and therefore could not be measured.

7. Concluding Remarks

By the proposed method, the concentration of atmospheric methane can be measured within an accuracy of 0.3 ppm•m, which is limited by the etalon fringes so far, but can be reduced to about 10 ppb•m employing more sophisticated optics. Now a portable equipment based on this method is in preparation for a field test.

Acknowledgements

The authors thank Mr.K.Shinohara of Fujitsu Laboratories,Ltd., who has supplied the tunable diode laser and infrared detectors. This reseach has been financially supported in part by the Nissan Science Foundation.

References

[1] D.W.Hill, and T.Powell, *Non-dispersive Infrared Gas Analysis in Science, Medicine and Industry*, Plenum Press, New York, 1968.

[2] W.F.Herget, J.A.Jahnke, D.E.Burch, and D.A.Gryvnak, Appl.Opt., **15**(1976)1222.

[3] J.Reid, J.Shewchun, B.K.Garside, and E.A.Ballik, Appl.Opt., **17** (1978)300.

[4] J.Reid, B.K.Garside, J.Shewchun, E.El-Sherbiny, and E.A. Ballik, Appl.Opt., **17**(1978)1806.

[5] D.T.Williams and R.N.Hager, Jr., Appl.Opt., **9**(1970)1597.

[6] R.N.Hager, Jr. and R.C.Anderson, J.Opt.Soc.Amer., **60**(1970)1444.

[7] A.R. Hawthorne and J.H. Thorngate, Appl. Opt., **17**(1978)742.
[8] H. Sano, R. Koga, Y. Tanada, and M. Kosaka, Memoirs of the School of Eng., Okayama Univ., **13**(1979)181.
[9] R. Koga, S. Nagase, M. Kosaka, and H. Sano, Memoirs of the School of Eng., Okayama Univ., **15**(1980), 1, 47.